Available online at www.sciencedirect.com
SCIENCE DIRECT®
International Journal of Heat and Mass Transfer 49 (2006) 240–250
International Journal of HEAT and MASS TRANSFER
www.elsevier.com/locate/ijhmt

Heat transfer of aqueous suspensions of carbon nanotubes (CNT nanofluids)

Yulong Ding *, Hajar Alias, Dongsheng Wen, Richard A. Williams

Institute of Particle Science and Engineering, University of Leeds, Leeds LS2 9JT, UK

Received 1 April 2005
Available online 27 September 2005

Abstract

This paper is mainly concerned about the heat transfer behaviour of aqueous suspensions of multi-walled carbon nanotubes (CNT nanofluids) flowing through a horizontal tube. Significant enhancement of the convective heat transfer is observed and the enhancement depends on the flow conditions (Reynolds number, *Re*), CNT concentration and the pH, with the effect of pH smallest. Given other conditions, the enhancement is a function of axial distance from the inlet, increasing first, reaching a maximum, and then decreasing with increasing axial distance. The axial position of the maximum enhancement increases with CNT concentration and *Re*. Given CNT concentration and the pH level, there appears to be a *Re* above which a big increase in the convective heat transfer coefficient occurs. Such a big increase seems to correspond to the shear thinning behaviour. For nanofluids containing 0.5 wt.% CNTs, the maximum enhancement reaches over 350% at $Re = 800$, which could not be attributed purely to the enhanced thermal conduction. Particle re-arrangement, shear induced thermal conduction enhancement, reduction of thermal boundary due to the presence of nanoparticles, as well as the very high aspect ratio of CNTs are proposed to be possible mechanisms.

Keywords: Nanofluids; Carbon nanotubes; Convective heat transfer; Effective thermal conductivity; Rheology; Entrance region

1. Introduction

Conventional heat transfer fluids such as air, helium, water, minerals oil, Freon, and ethylene glycol play an important role in a number of industrial sectors including power generation, chemical production, air-conditioning, transportation and microelectronics. These fluids, however, are inadequate for high heat flux applications such as superconducting magnets, super-fast computing and high power microwave tubes due to restrictions of their thermal properties such as conductivity. Numerous investigations have therefore been carried out in the past few decades, seeking to develop novel methods for enhancing the thermal performance of heat transfer fluids. One of the methods is the incorporation into the base liquid high thermally conductive particulate solids such as metals or metal oxide; see for example [26,1,2,14]. These early studies, however, used suspensions of millimeter or micrometer sized particles, which, although showed some enhancement, experienced problems such as abrasion and channel clogging due to poor suspension stability particularly in the case of mini- and/or micro-channels. A recent invention

* Corresponding author. Tel.: +44 113 343 2747; fax: +44 113 243 2405.
E-mail address: y.ding@leeds.ac.uk (Y. Ding).

0017-9310/$ - see front matter © 2005 Elsevier Ltd. All rights reserved.
doi:10.1016/j.ijheatmasstransfer.2005.07.009

Nomenclature

A	tube cross-sectional area
D	tube diameter
c_p	fluid heat capacity
d_p	particle diameter
h	heat transfer coefficient
k	fluid thermal conductivity
Nu	Nusselt number
Pe	Peclet number, $\dot{\gamma} \cdot d_p^2/v$
Pr	Prandtl number
q	heat flux
Re	Reynolds number $Re = \rho u D/\mu$
S	perimeter of tube
T	temperature
u	fluid velocity
x	axial distance

Greek symbols

α	fluid thermal diffusivity
δ_t	thermal boundary layer thickness
$\dot{\gamma}$	fluid shear rate
v	fluid kinematic viscosity
μ	fluid dynamic viscosity
ρ	fluid density

Subscripts

f	fluid
in	inlet
w	wall

termed 'nanofluids' has shown potential to resolve some disadvantages associated with the suspensions of large particles [5]. Nanofluids are liquid suspensions containing particles that are significantly smaller than 100 nm in at least one dimension, and have bulk thermal conductivities orders of magnitudes higher than the base liquids. The advantages of *properly* engineered nanofluids include (a) higher thermal conductivities than that predicted by currently available macroscopic models, (b) excellent stability, and (c) little penalty due to an increase in pressure drop and pipe wall abrasion experienced by suspensions of millimeter or micrometer particles. As a result of these advantages, a number of studies have been performed on the thermal properties of nanofluids since the invention approximately a decade ago; see for examples [22,5,12,20,36,13,15,34,28–30]. These studies are mostly on the effective thermal conductivity under macroscopically static conditions, and only small number of studies have been carried out on the other aspects such as phase change behaviour [7–9,40,27,32] and convective heat transfer [19,23,37,21,38,16,31].

This work is concerned about the convective heat transfer of suspensions of carbon nanotubes (CNT nanofluids). The motivations behind are: (a) No previous studies have been found in the literature on the convective heat transfer of CNT nanofluids; (b) Very high thermal conductivity of cabon nanotubes and hence great potential for significant heat transfer enhancement (~3000 W/m K for multi-walled CNTs [18] and ~6000 W/m K for single walled CNTs [4]); and (c) There are inconsistencies in the few reported studies on the convective heat transfer using nanofluids [23,38,39,31].

This paper is organised in the following manner. Section 2 describes the details of experimental systems and materials used. Experimental results are presented and discussed in Section 3. Section 4 summarises the main conclusions. Reviews of relevant work in the literature will also be included where appropriate.

2. Experimental

2.1. Materials and nanofluids preparation

Distilled water and multi-walled carbon nanotubes were used to produce nanofluids. The carbon nanotubes (CNT) were provided by the Tsinghua Nafine Nanopowder Commercialization Engineering Centre (China) and were used as received. They were produced catalytically from hydrocarbon materials on nano-catalyst under high pressures. Fig. 1(a) and (b) show respectively an SEM image and a TEM image of the sample. It can be seen that the nanotubes are entangled and some are in the format of agglomerates.

It is known that CNTs have a hydrophobic surface, which is prone to aggregation and precipitation in water in the absence of a dispersant/surfactant [41]. Lots of efforts were therefore made in the initial stage of the work, searching for an appropriate dispersant. After many trial and error tests, sodium laurate (SL), sodium dodecyl benzene sulfonate (SDBS) and gum Arabic (GA) were found to be able to stabilise carbon nanotubes for more than a month without visually observable sedimentation. As SDBS was observed to fail at elevated temperatures [30], GA purchased from Beecroft Scientific (UK) was used as the dispersant in this work. As mentioned above, CNTs are entangled and some are in the form of agglomerates, measures are needed to disentangle nanotubes and to break agglomerates. The methods used in this work included ultrasonification of carbon nanotubes under dry conditions and high shear

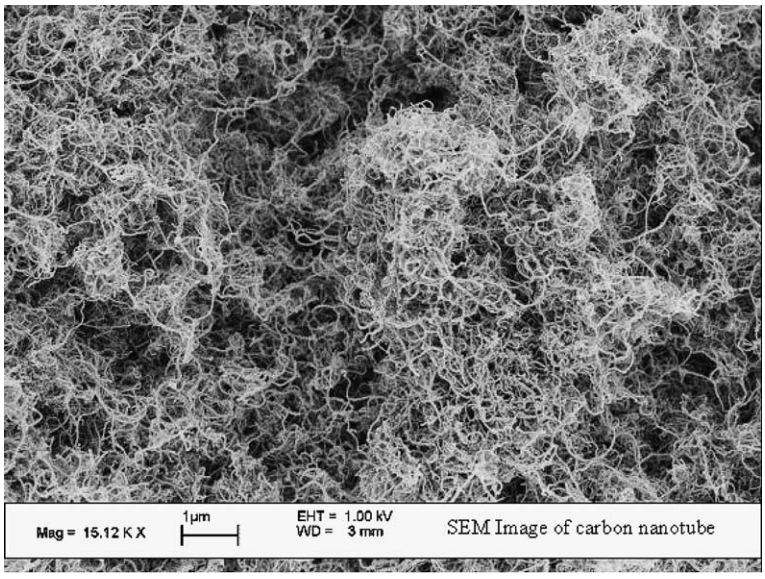

(a)

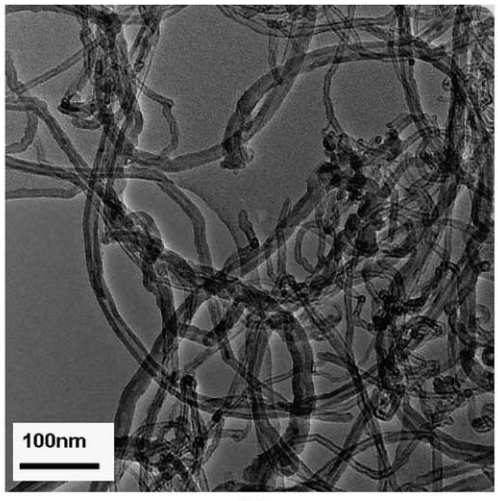

(b)

Fig. 1. Images of carbon nanotubes as received: (a) SEM image of carbon nanotubes and (b) TEM image of carbon nanotubes.

homogenisation of the dispersion. The homogenization was realised by using an Ultra-Turrax T25 mixer (IKA, Germany). The mixer had a gap of 0.5 mm between the rotor and the stator. The rotational speed of the rotor was adjustable and the highest speed was ~24,000 rpm, which could provide a shear rate up to 40,000 s^{-1} and opportunities to break agglomerates.

A typical process for nanofluids preparation involves in series (a) sonicating a CNT sample with a known weight in an ultrasonic bath for over 24 h, (b) dispersing the sonicated CNTs into a preset amount of distilled water containing Gum Arabic dispersant and adjusting the suspension to a preset pH level, and (c) treating the mixture with the high shear homogeniser for 30 min. CNT nanofluids made in this way were found to be very stable for months without visually observable sedimentation. Fig. 2 shows a SEM image of the dispersed sample. It can be seen that carbon nanotubes have largely been disentangled.

2.2. Measurements of the effective thermal conductivity and viscosity of CNT nanofluids

Assessment of the convective heat transfer performance requires the effective thermal conductivity and

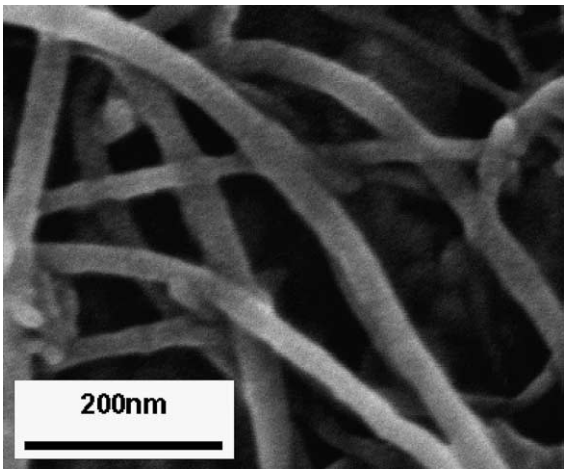

Fig. 2. SEM image of a dispersed sample of carbon nanotubes.

viscosity. The thermal conductivity was measured by using a KD2 thermal property meter (Labcell Ltd., UK), which is based on the transient hot wire method. The KD2 meter has a probe with 60 mm length and 0.9 mm diameter, which integrates in its interior a heating element and a thermo-resistor, and is connected to a microprocessor for controlling and conducting the measurements. The KD2 meter was calibrated by using distilled water before any set of measurements. In order to study the effect of temperature on the effective thermal conductivity of nanofluids, a thermostat bath (GD120-S12, Grant, UK) was used, which was able to maintain temperature uniformity within ± 0.02 K. At least five measurements were taken for each CNT concentration at a given temperature to ensure the uncertainty of measurements within 3%. The viscosity was measured by using a Bohlin CVO rheometer (Malvern Instruments, UK). The measurements were done on nanofluids of different CNT concentrations at a shear rate between ~ 0.3 and 10 000 s^{-1}. To assess the effect of the presence of the dispersant, several measurements were also carried out on the gum Arabic–water solutions under the same shear rate range.

2.3. Experimental system and principle for measuring the convective heat transfer coefficient

The experimental system for measuring the convective heat transfer coefficient is similar to the one used by Wen and Ding [31], and is shown schematically in Fig. 3. It consisted of a flow loop, a heat unit, a cooling part, and a measuring and control unit. The flow loop included a pump with a built-in flowmeter, a reservoir, a collection tank and a test section. A straight copper tube with 970 mm length, 4.5 mm inner diameter, and 6.35 mm outer diameter was used as the test section. The whole test section was heated by a flexible silicon rubber heater (Watlow, UK) linked to a DC power supply (TTi Ex752m, RS, UK). The power supply was adjustable and had a maximum power supply of 300 W. There was a thick thermal isolating layer surrounding the heater to obtain a constant heat flux condition along the test section. Five T-type thermocouples were mounted on the test section at axial positions in mm of 118 (T1), 285 (T2), 524 (T3), 662 (T4) and 782 (T5) from the inlet of the test section to measure the wall temperature distribution, and two further T-type thermocouples were inserted into the flow at the inlet and exit of the test section to measure the bulk temperatures of nanofluids. The pump used in this work was of peristaltic type with the flowrate controlled by the rotational rate. The maximum flow rate the pump could deliver was 10 l min^{-1}. There was a three-way valve in the flow

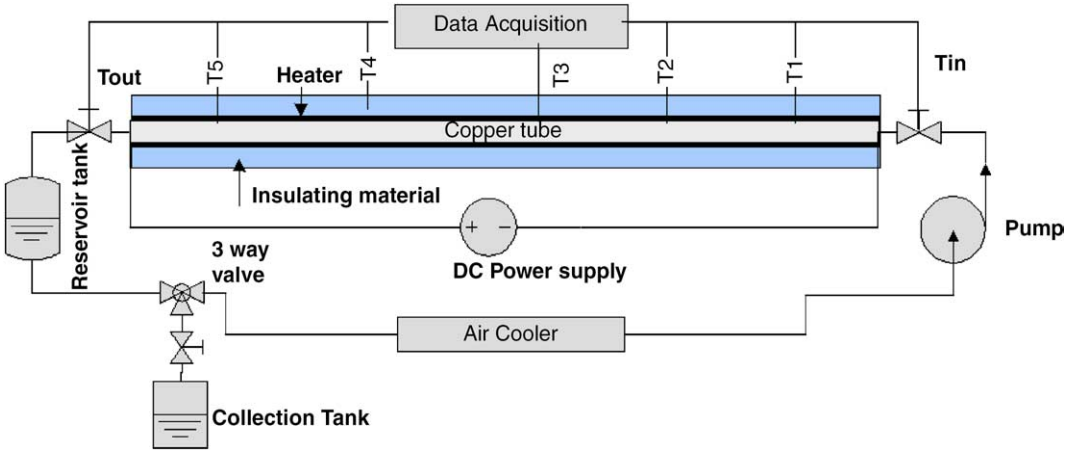

Fig. 3. Experimental system.

loop for flowrate calibrations and flow system cleaning between runs even with the same nanofluid. In the heat transfer experiments, the pump rotational rate, voltage and current of the DC power supply were recorded and the temperature readings from the 7 thermocouples were registered by a data requisition system. As the pump performance was sensitive to the fluid viscosity at a given rotational speed, calibration was needed, which was carried out before and after each experiment by a weighing method. This gave an accuracy of nanofluids flowrate better than 4.6%. The thermocouples were calibrated in a thermostat water bath and the accuracy was found to be within 0.1 K.

The convective heat transfer coefficient (h) is defined as

$$h(x) = q/(T_w(x) - T_f(x)) \quad (1)$$

where x represents axial distance from the entrance of the test section, q is the heat flux, T_w is the measured wall temperature, and T_f is the fluid temperature decided by the following energy balance:

$$T_f(x) = T_{in} + qSx/(\rho c_p u A) \quad (2)$$

where c_p is the heat capacity, ρ is the fluid density, A and S are respectively the cross-sectional area and perimeter of the test tube, and u is the average fluid velocity. Eq. (2) is based on an assumption of zero heat loss through the insulation layer. The deviation to this assumption was assessed by comparing the measured temperature difference between inlet and outlet of the test section with the theoretical value calculated by Eq. (2). It was found that the maximum deviation was lower than 6.2% under the conditions of this work.

The convective heat transfer coefficient, h, in Eq. (1) is usually expressed in the form of the Nusselt number (Nu) as:

$$Nu(x) = h(x)D/k \quad (3)$$

where D is the tube diameter, and k is the fluid thermal conductivity. Traditionally, the Nu number is related to the Reynolds number defined as $Re = \rho u D/\mu$ and the Prandtl number defined as $Pr = \nu/\alpha$, where ν is the fluid kinematic viscosity, α is the fluid thermal diffusivity, and μ the fluid dynamic viscosity.

3. Results and discussion

3.1. Effective thermal conductivity

Fig. 4 shows the effective thermal conductivity of nanofluids as a function of CNT concentration at three temperatures. The concentration of gum Arabic was 0.25 wt.% with respect to water, which was found to give excellent stability to the CNT nanofluids. It can be seen that the effective thermal conductivity increases with increasing temperature and CNT concentration, with the dependence of the conductivity on temperature much more significant. At 20 and 25 °C, the dependence of the effective thermal conductivity levels off at CNT concentrations greater than ~0.5 wt.%, while this does not occur at 30 °C. The enhancement of the thermal conductivity shown in Fig. 4 is slightly higher than that reported by Assael et al. [3], Xie et al. [35], and Wen and Ding [30], but much lower than that reported by Choi et al. [6]. The exact reason for this discrepancy is unclear but is believed to be associated with the thermal properties of CNTs used, liquid-CNT interfacial resistance, and the aspect ratio of CNTs used [10,30]. It should be noted that the base liquid used by Choi et al. [6] is oil, which has a much lower thermal conductivity than water; therefore the absolute increase in conductivity is not huge.

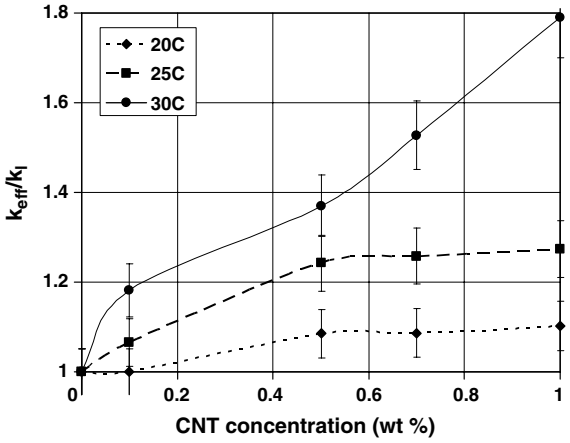

Fig. 4. Measured thermal conductivity of CNT nanofluids under different conditions: gum Arabic concentration 0.25 wt.% with respect to water.

3.2. Viscosity of nanofluids

The viscosity of CNT nanofluids as a function of shear rate was measured under various conditions. Shown in Fig. 5(a) are results for two different temperatures and concentrations at pH = 6. A clear shear thinning behavior is seen under all conditions. At a given shear rate, the viscosity of nanofluids increases with increasing CNT concentration and decreasing temperature. The shear thinning behaviour was also observed by Kinloch et al. [17] for highly concentrated aqueous suspensions of multiwalled carbon nanotubes. The results shown in Fig. 5(a) have very an important implication to CNT nanofluids flowing through the tubular geometry used in this work as the shear rate at the wall region is higher than that at the core region, hence lower viscosity at the wall region and better lubrication effect.

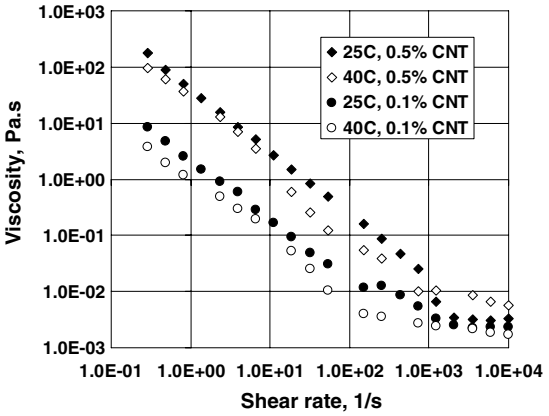

(a) Viscosity of CNT nanofluids (pH=6.0)

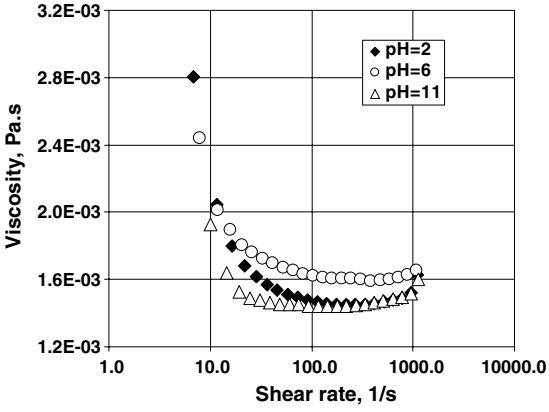

(b) Viscosity of gum Arabic – water solution (25°C)

Fig. 5. Viscosity as a function of shear rate for: (a) CNT nanofluids and (b) gum Arabic solutions: 0.25% gum Arabic in all formulations.

The results also bear important implications to heat transfer as the heat transfer coefficient depends on the flow behaviour. More discussion will be made in the Section 3.3. There may be doubts that the shear thinning behaviour is due to the presence of gum Arabic dispersant. A few rheological experiments were therefore carried out on gum Arabic solutions. The results are illustrated in Fig. 5(b), which clearly shows the shear thinning behaviour at low shear rates but slight shear thickening is seen at shear rates greater than $\sim$200 s^{-1}. A comparison of Fig. 5(a) and (b) shows that, at low shear rates, the viscosity of gum Arabic solutions is several orders of magnitude lower than that of the CNT nanofluids. The gap is narrowed down at high shear rates but the difference is still several-folds. This suggests that the presence of gum Arabic affects little on the viscosity of CNT nanofluids at low shear rates but may play a role at high shear rates. Further discussion will be made in Section 3.3.

3.3. Convective heat transfer coefficient

3.3.1. Convective heat transfer coefficient of pure water

Before conducting systematic experiments with CNT nanofluids, the reliability and accuracy of the experimental system were tested using distilled water as the working fluid. The results are shown in Fig. 6, together with predictions of the following well-known Shah equation for laminar flows under the constant heat flux boundary condition [25]:

$$Nu = \begin{cases} 1.953\left(RePr\dfrac{D}{x}\right)^{1/3} & \left(RePr\dfrac{D}{x}\right) \geqslant 33.3 \\ 4.364 + 0.0722RePr\dfrac{D}{x} & \left(RePr\dfrac{D}{x}\right) < 33.3 \end{cases} \tag{4}$$

Reasonably good agreement has been achieved between the Shah equation and the measurements over the Reynolds number range used in this work.

3.3.2. Convective heat transfer coefficient of CNT nanofluids

Having established confidence in the experimental system, systematic experiments were performed at different flow conditions (Reynolds numbers), different CNT concentrations, and pH levels. The results are presented and discussed in this sub-section. As the viscosity is not well defined due to non-uniform shear rate across the pipe cross section, the Reynolds number is calculated based on the viscosity of the host liquid at zero-shear rate. However, it may be possible to use an alternative non-dimensionless group based on non-Newtonian models for the viscosity to replace the Reynolds number as described above. This is currently under investigation.

3.3.2.1. Effect of CNT concentration on the convective heat transfer. Fig. 7(a) shows the effect of CNT

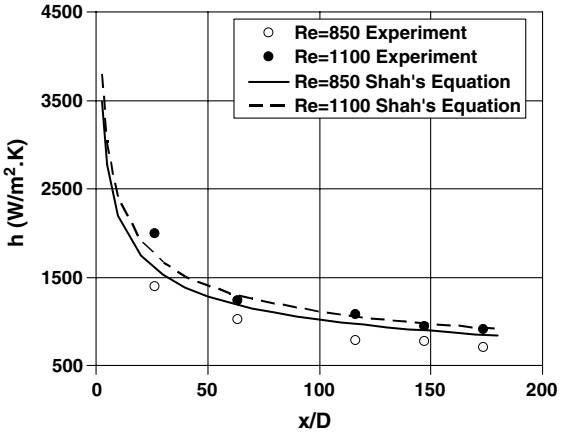

Fig. 6. Initial test of the experiment rig using distilled water.

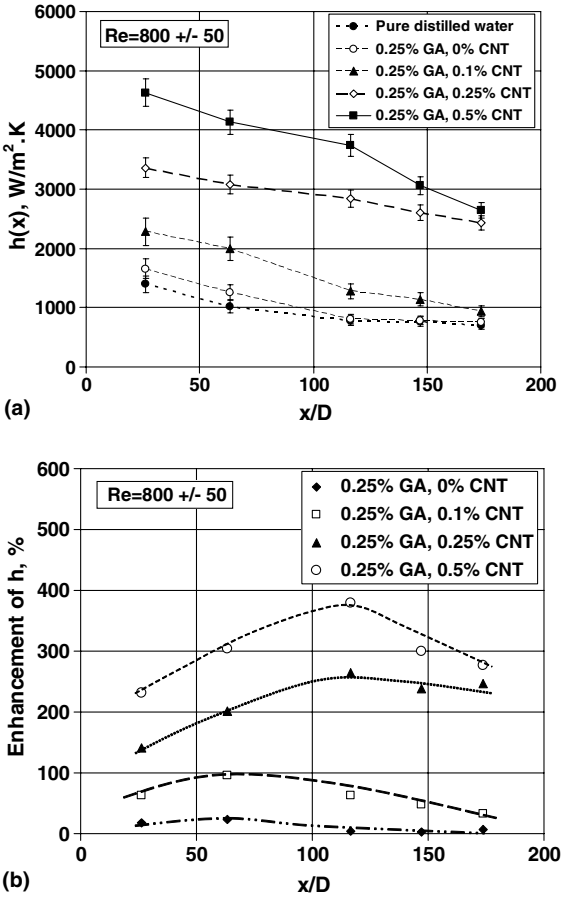

Fig. 7. Axial profiles of heat transfer coefficient (a) and enhancement of heat transfer coefficient (b) for different CNT concentrations (pH = ~6).

concentration on the local heat transfer coefficient at various axial distances from the entrance of the test section at $Re = 800 \pm 50$ and pH = 6. Also included in the figure are the results of pure distilled water and gum Arabic–water solution for comparison purposes. Fig. 7(b) shows the enhancement of the heat transfer coefficient, with reference to pure distilled water, as a function of axial distance at different CNT concentrations. The following observations can be made from the two figures:

- The presence of gum Arabic only gives a marginal enhancement on the heat transfer performance at $x/D < \sim 100$, but the enhancement approaches to zero at $x/D > \sim 100$ (Fig. 7a and b).
- The presence of carbon nanotubes increases the convective heat transfer coefficient significantly, and the increase is more considerable at high CNT concentrations (Fig. 7a).
- At a given CNT concentration, the heat transfer coefficient decreases with axial distance (Fig. 7a). This is as expected for heat transfer in the entrance region; see later for more discussion.
- The enhancement of heat transfer coefficient increases with x/D initially, reaches a maximum at a value of x/D depending on CNT concentration, and then decreases with a further increase in x/D. The value of x/D at which the enhancement is maximum increases with CNT concentration (Fig. 7b).

Fig. 7(a) and (b) suggest a possible smart measure to keep the high heat transfer coefficient—creation of many 'artificial entrance' regions along a pipeline. The use of artificial length will inevitably increase the pressure drop hence optimisation is needed. This will be one of the objectives for our future work.

A comparison of Fig. 7 with Fig. 4 indicates that the enhancement of the convective heat transfer coefficient is much more dramatic than that purely due to the enhancement of effective thermal conductivity. A similar trend but with less significant enhancement was also observed by Xuan and Li [38] in the turbulent flow regime and Wen and Ding [31] at the entrance region in the laminar flow regime. Xuan and Li [38] showed that the heat transfer coefficient was increased by ~60% for an aqueous based nanofluid containing 2% Cu nanoparticles by volume, but the nanofluid only had an effective thermal conductivity approximately 12.5% higher than that of the base liquid. Wen and Ding [31] investigated heat transfer of aqueous γ-alumina nanofluids and observed a ~47% increase in the convective heat transfer coefficient at $x/D \sim 60$ for 1.6 vol.% nanoparticle loading and $Re = 1600$, which was much greater than that due to the enhancement of thermal conduction (<~10%). More discussion on this will be made later.

3.3.2.2. Effect of Reynolds number (flow condition) on the convective heat transfer. Fig. 8(a) shows the effect of the Reynolds number, which clearly indicates that the heat transfer coefficient increases with increasing Reynolds number. There is a large difference between the heat transfer coefficient at $Re = 1200$ and that at $Re <$ ~1100, which will be discussed in the following. Fig. 8(b) shows the enhancement of the heat transfer coefficient with reference to pure water. It can be seen that the heat transfer enhancement increases with increasing Reynolds number at $Re = 1000$–1200, but a more complex case occurs at $Re = 800$. At $x/D <$ ~110, the enhancement for $Re = 800$ is higher than that for $Re = 1000$ and 1100, but this is reversed at $x/D >$ ~110. To identify how the heat transfer enhancement changes with Reynolds number, the data shown in Fig. 8(b) are presented in a different format in Fig. 9. It is seen that the effect of Reynolds number is small at $Re <$ ~1100 but a big increase occurs when the Reynolds number becomes greater than 1100. The exact reason for this requires further investigation, but the

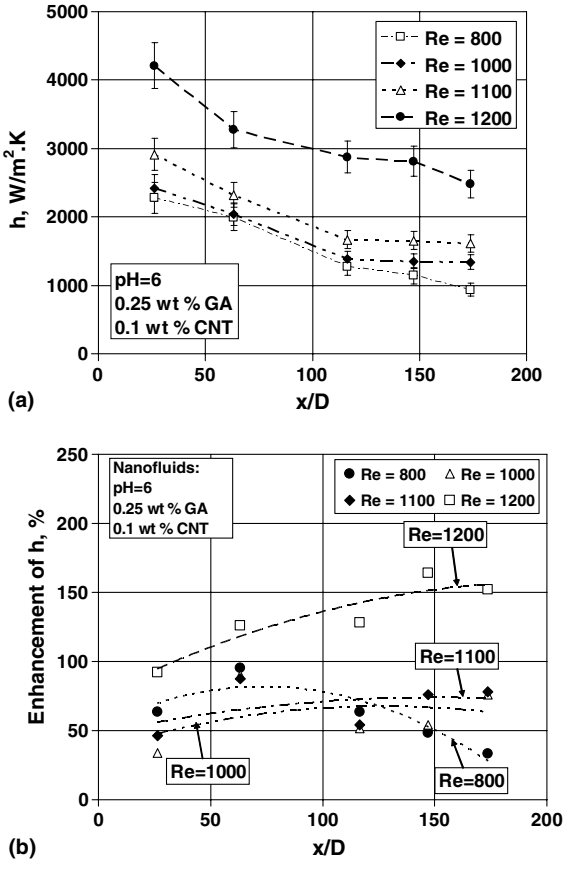

Fig. 8. Effect of Reynolds number on the convective heat transfer coefficient (a) and heat transfer enhancement (b) for 0.1 wt.% CNT at pH = 6.

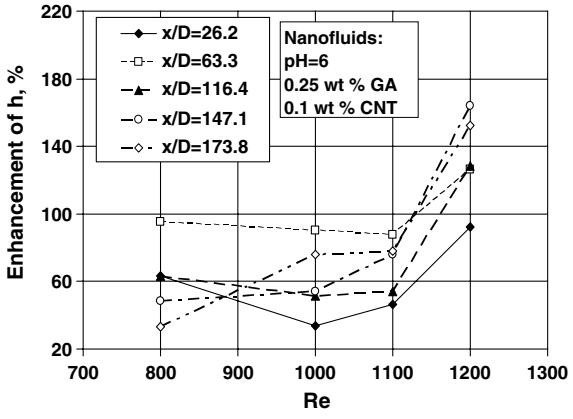

Fig. 9. Enhancement of heat transfer coefficient as a function of Reynolds number at different axial positions.

effect of shear rate on the viscosity could be a reason. At $Re = 1100$, the shear rate at the wall is approximately $500\ s^{-1}$, which corresponds to the transition from the strong shear thinning region to the region with approximately constant viscosity. More experiments are needed to confirm this suggestion.

It is recognised that measurements of pressure drop across the tube length under different conditions could provide some information for relating directly the observed heat transfer behaviour to the flow behaviour. This is currently under consideration.

3.3.2.3. Effect of pH on the convective heat transfer. Fig. 10 compares the axial profiles, at two Reynolds numbers, of the convective heat transfer coefficient under two pH conditions. The convective heat transfer coefficient at pH = 6 is slightly higher than that at pH = 10.5. It is unclear if the effect of pH is actually very small under other pH conditions. Further work is underway and will be reported in the future. If the small effect of pH is proven, excellent opportunities will be provided for future industrial taking-up of the technology as both very acidic and basic suspensions would increase both the capital and operating costs and also have significant safety implications.

3.3.2.4. Mechanisms of heat transfer enhancement. The heat transfer coefficient, h, is a macroscopic parameter describing heat transfer when a fluid flowing across a solid surface of different temperature. It is not a material property but can be approximately given by k/δ_t with δ_t the thickness of thermal boundary layer. At the entrance ($x/D = 0$), the theoretical boundary layer thickness is zero, hence the heat transfer coefficient approaches infinity. The boundary layer increases with axial distance until fully developed after which the boundary layer thickness and hence the convective heat transfer

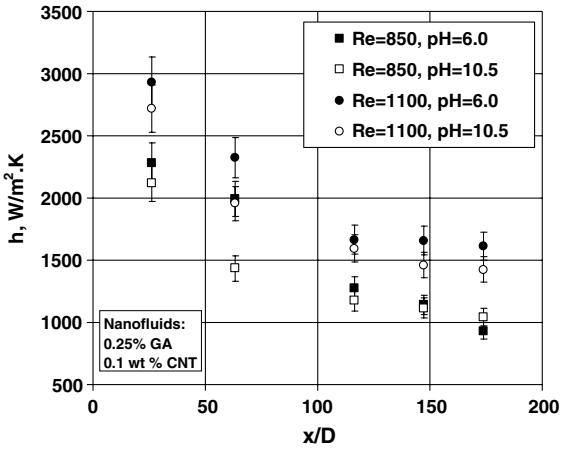

Fig. 10. Effect of pH on the convective heat transfer.

coefficient is constant. The above simple argument (from heat transfer textbooks) only addresses the problem qualitatively, but give little insight into the mechanisms for the observed large heat transfer enhancement. However, it does provide a starting point for looking at possible underlying mechanisms.

The above simplified theory suggests that both an increase in k and/or a decrease in δ_t increase the convective heat transfer coefficient. As can be seen from Fig. 4, the maximum enhancement of the thermal conductivity under the conditions of the convective heat transfer experiments in this work does not exceed 18% for 0.1% CNT nanofluids and 37% for 0.5% CNT nanofluids. The enhancement of the convective heat transfer coefficient, however, is much greater than that due to the increase in the thermal conductivity, particularly at high CNT concentrations and high Reynolds numbers; see Figs. 7–9. One may therefore simply attribute the large enhancement purely to a decrease in the thermal boundary layer thickness. No doubt, the reduction in the thermal boundary layer thickness could be an important factor, but further enhancement on the thermal conduction under dynamic conditions could be another important factor. The effective thermal conductivity shown in Fig. 4 is obtained under the static conditions, whereas significant shear exists under the conditions of the convective heat transfer experiments. As shown in Fig. 5, CNT nanofluids exhibit a significant shear thinning behaviour, the effective thermal conductivity under dynamic shear conditions may therefore be much higher than that shown in Fig. 4. Such behaviour has indeed been observed previously by Sohn and Chen [26] who measured the effective thermal conductivity in a rotating Couette flow apparatus at low Reynolds number but high Peclet number conditions, where the Peclet number is defined as $\dot{\gamma} \cdot d_p^2/v$ with $\dot{\gamma}$ the shear rate, and d_p particle diameter. Significant enhancement on the effective thermal conductivity was observed at Peclet numbers over 300, and the shear-dependent behaviour fitted well into a power law relationship. A similar trend was also reported by Ahuja [1], who used a shell-and-tube heat exchanging arrangement, and employed the Graetz solutions at the entrance region to evaluate the effective thermal conductivity of a saline/polystyrene latex suspension. These researchers attributed the enhancement to the high Peclet number, which represents a measure of the eddy scale convection as compared to conduction, and therefore is associated with self-rotating and/or micro-convection [1,2]. For CNT nanofluids, Peclet number is of an order of 1 under the conditions of this work if the shear rate at the wall and the volume based equivalent particle diameter are used in the calculation. This seems to suggest little contribution of enhanced thermal conduction to the observed large enhancement of the convective heat transfer coefficient. However, CNTs are likely to form structures, which may have an effective particle size much larger than the volume based equivalent particle diameter, and hence lead to a much higher Peclet number and significant further enhancement on the thermal conduction.

As shown in Figs. 7–10, the convective heat transfer coefficient decreases with axial distance, and the decay for pure water is much quicker than that for CNT nanofluids. This indicates that the presence of CNTs affects the development of boundary layers. The effect of particles on the boundary layer development has also been suggested to be the main mechanism for heat transfer enhancement in particulate flows under the turbulent flow regime [14]. For a pure Newtonian fluid flowing in a straight pipe, the boundary layer develops smoothly and the flow is hydrodynamically and thermally fully developed at $x/D \geqslant \sim(0.05Re)$ and $x/D \geqslant \sim(0.05RePr)$, respectively. The criterion for the thermal boundary layer development obviously does not apply to CNT nanofluids as clearly shown in Figs. 7–10. Further work is needed in this aspect. The above discussion is mostly from the macroscopic point of view. Microscopically, particle migration and re-arrangement due to non-uniform shear rate over the pipe cross-section could also be a reason for the observed large heat transfer enhancement. In normal pipe flows, the highest shear rate occurs at the wall, whereas the lowest shear rate takes place at the centre. The non-uniform shear rate implies non-uniformity in both viscosity and thermal conductivity; see Refs. [24,11,33]. Wen and Ding [33], by using a theoretical model, showed that the non-uniform thermal conductivity profile resulting from particle migration could lead to a higher Nusselt number.

A final point is the effect of particle shape on the heat transfer performance. Previous studies using nearly spherical nanoparticles by Pak and Cho [23], Xuan and Li [38] and Wen and Ding [31] showed an enhancement of the convective heat transfer of up to ~60%. Recently, Yang et al. [39] studied the laminar flow heat transfer of nanofluids made from disc-like graphitic nanoparticles with an aspect ratio of ~0.02. They found very small enhancement in the heat transfer coefficient, and the enhancement is even lower than that due to thermal conductivity. These observations seem to suggest that the observed high heat transfer enhancement in this work be (at least partially) associated with the very high aspect ratio (>100) of CNTs. More work is needed to confirm this.

In summary, the observed large enhancement of the convective heat transfer coefficient is associated with (a) enhancement of the thermal conductivity under the static conditions, (b) further enhancement on the thermal conduction under the dynamic conditions (shear induced), (c) reduction of the boundary layer thickness and delay in the boundary layer development, (d) particle re-arrangement due to non-uniform shear-rate across the pipe cross-section, and (e) high aspect ratio of CNTs.

4. Conclusions

This paper reports a recent study on the heat transfer behaviour of aqueous suspensions of multi-walled carbon nanotubes (CNT nanofluids). Stable CNT nanofluids are produced by using both ultrasonification and high shear homogenisation methods in the presence of a small percentage of gum Arabic. Systematic experiments are performed on the produced nanofluids to obtain the effective thermal conductivity, viscosity and convective heat transfer coefficient. The following conclusions are obtained:

- Significant enhancement is observed of the convective heat transfer in comparison with pure water as the working fluid. The enhancement depends on the flow condition, CNT concentration and the pH level, and the effect of pH is observed to be small.
- Given other conditions, the enhancement is a function of the axial distance from the inlet of the test section; the enhancement increases first, reaches a maximum, and then decreases with increasing axial distance. The position at which the maximum enhancement occurs increases with CNT concentration and the Reynolds number.
- Given CNT concentration and pH level, there seems to be a Reynolds number above which a big increase in the convective heat transfer coefficient occurs. Such a big increase is likely to correspond to the shear thinning behaviour.
- For nanofluids containing 0.5 wt.% CNTs, the maximum enhancement is over 350% at $Re = 800$, and the maximum enhancement occurs at an axial distance of approximately 110 times the tube diameter.
- The observed large enhancement of the convective heat transfer could not be attributed purely to the enhancement of thermal conduction under the static conditions. Particle re-arrangement, shear induced thermal conduction enhancement, reduction of thermal boundary layer thickness due to the presence of nanoparticles, as well as the very high aspect ratio of CNTs are proposed to be possible mechanisms.

Acknowledgement

The authors are grateful to the Tsinghua Nafine Nano-powder Commercialization Engineering Centre, China, for providing carbon nanotubes.

References

[1] A.S. Ahuja, Augmentation of heat transport in laminar flow of polystyrene suspension: I—experiments and results, J. Appl. Phys. 46 (1975) 3408–3416.
[2] A.S. Ahuja, Augmentation of heat transport in laminar flow of polystyrene suspension: II—analysis of data, J. Appl. Phys. 46 (1975) 3417–3425.
[3] M.J. Assael, C.F. Chen, I. Metaxa, W.A. Wakeman, Thermal conductivity of suspensions of carbon nanotubes in water, paper presented to the 15th Symposium on Thermophysical Properties, National Institute of Standards, University of Colorado, Boulder, USA, 22–27 June, 2003.
[4] S. Berber, Y.K. Kwon, D. Tomanek, Unusually high thermal conductivity of carbon nanotubes, Phys. Rev. Lett. 84 (2000) 4613–4616.
[5] S.U.S. Choi, Enhancing thermal conductivity of fluids with nanoparticles, in: D.A. Siginer, H.P. Wang (Eds.), Developments Applications of Non-Newtonian Flows, FED-vol. 231/MD-vol. 66, ASME, New York, 1995, pp. 99–105.
[6] S.U.S. Choi, Z.G. Zhang, W. Yu, F.E. Lockwood, E.A. Grulke, Anomalous thermal conductivity enhancement in nanotube suspensions, Appl. Phys. Lett. 79 (14) (2001) 2252–2254.
[7] S.K. Das, N. Putra, W. Roetzel, Pool boiling characteristics of nano-fluids, Int. J. Heat Mass Transfer 46 (2003) 851–862.
[8] S.K. Das, N. Putra, W. Roetzel, Pool boiling of nanofluids on horizontal narrow tubes, Int. J. Multiphase Flow 29 (2003) 1237–1247.
[9] S.K. Das, N. Putra, P. Thiesen, W. Roetzel, Temperature dependence of thermal conductivity enhancement for nanofluids, ASME J. Heat Transfer 125 (2003) 567–574.
[10] Y.L. Ding, D.S. Wen, R.A. Williams, Nanofluids for heat transfer intensification—where are we ad where should we go? in: B.X. Wang (Ed.) Proceedings of the 6th International Symposium on Heat Transfer, Beijing, China, 2004, pp. 66–76.
[11] Y.L. Ding, D.S. Wen, Particle migration in a flow of a suspension of nanoparticles (nanofluids), Powder Technol. 149 (2004) 84–92.
[12] J.A. Eastman, S.U.S. Choi, S. Li, L.J. Thompson, S. Lee, Enhanced thermal conductivity through the development of nanofluids, in 1996 Fall meeting of the Materials Research Society (MRS), Boston, USA, 1996.
[13] J.A. Eastman, S.U.S. Choi, S. Li, W. Yu, L.J. Thompson, Anomalously increased effective thermal conductivities of ethylene glycol-based nanofluids containing copper nanoparticles, Appl. Phys. Lett. 78 (2001) 718–720.
[14] G. Hetsroni, R. Rozenblit, Heat transfer to a liquid–solid mixture in a flume, Int. J. Multiphase Flow 20 (1994) 671–689.
[15] P. Keblinski, S.R.E. Phillpot, S.U.S. Choi, J.A. Eastman, Mechanisms of heat flow in suspensions of nano-sized particles (nanofluids), Int. J. Heat Mass Transfer 45 (2002) 855–863.
[16] K. Khanafer, K. Vafai, M. Lightstone, Buoyancy-driven heat transfer enhancement in a two-dimensional enclosure utilizing nanofluids, Int. J. Heat Mass Transfer 46 (2003) 3639–3653.
[17] I.A. Kinloch, S.A. Roberts, A.H. Windle, A rheological study of concentrated aqueous nanotube dispersions, Polymer 43 (2002) 7483–7491.
[18] P. Kim, L. Shi, A. Majumdar, P.L. McEuen, Thermal transport measurements of individual multiwalled nanotubes, Phys. Rev. Lett. 87 (21) (2001) 215502.

[19] S. Lee, S.U.S. Choi, Application of metallic nanoparticle suspensions in advanced cooling systems, in: 1996 international mechanical engineering congress and exhibition, Atlanta, USA, 1996.
[20] S. Lee, S.U.S. Choi, S. Li, J.A. Eastman, Measuring thermal conductivity of fluids containing oxide nanoparticles, J. Heat Transfer, Trans. ASME 121 (1999) 280–289.
[21] Q. Li, Y.M. Xuan, Convective heat transfer and flow characteristics of Cu–water nanofluids, Sci. China, Series E 45 (2002) 408–416.
[22] H. Masuda, A. Ebata, K. Teramae, N. Hishinuma, Alteration of thermal conductivity and viscosity of liquid by dispersing ultra-fine particles (dispersion of γ-Al_2O_3, SiO_2 and TiO_2 ultra-fine particles), Netsu Bussei (Japan) 4 (1993) 227–233.
[23] B.C. Pak, Y.I. Cho, Hydrodynamic and heat transfer study of dispersed fluids with submicron metallic oxide particles, Experiment. Heat Transfer 11 (1999) 151–170.
[24] R.J. Phillips, R.C. Armstrong, R.A. Brown, A.L. Graham, J.R. Abbott, A constitutive equation for concentrated suspensions that accounts for shear-induced particle migration, Phys. Fluids A 4 (1992) 30–40.
[25] R.K. Shah, Thermal entry length solutions for the circular tube and parallel plates, in: Proc. 3rd National Heat Mass Transfer Conference. Indian Institute of Technology, Bombay, 1, Paper no. HMT-11-75, 1975.
[26] C.W. Sohn, M.M. Chen, Microconvective thermal conductivity in disperse two phase mixture as observed in a low velocity Couette flow experiment, J. Heat Transfer, Trans. ASME 103 (1981) 47–51.
[27] P. Vassallo, R. Kumar, S. Damico, Pool boiling heat transfer experiments in silica-water nano-fluids, Int. J. Heat Mass Transfer 47 (2004) 407–411.
[28] X.W. Wang, X.F. Xu, S.U.S. Choi, Thermal conductivity of nanoparticle–fluid mixture, J. Thermophys. Heat Transfer 13 (1999) 474–480.
[29] B.X. Wang, L.P. Zhou, X.F. Peng, A fractal model for predicting the effective thermal conductivity of liquid with suspension of nanoparticles, Int. J. Heat Mass Transfer 46 (2003) 2665–2672.
[30] D.S. Wen, Y.L. Ding, Effective thermal conductivity of aqueous suspensions of carbon nanotubes (Nanofluids), J. Thermophys. Heat Transfer 18 (4) (2004) 481–485.
[31] D.S. Wen, Y.L. Ding, Experimental investigation into convective heat transfer of nanofluids at entrance area under laminar flow region, Int. J. Heat Mass Transfer 47 (24) (2004) 5181–5188.
[32] D.S. Wen, Y.L. Ding, Experimental investigation into the pool boiling heat transfer of aqueous based γ-Alumina nanofluids, J. Nanoparticle Research 7 (2005) 265–274.
[33] D.S. Wen, Y.L. Ding, Effect on heat transfer of particle migration in suspensions of nanoparticles flowing through minichannels, Microfluidics and Nanofluidics 1 (2) (2005) 183–189.
[34] H. Xie, J. Wang, T.G. Xi, Y. Liu, F. Ai, Thermal conductivity enhancement of suspensions containing nanosized alumina particles, J. Appl. Phys. 91 (2002) 4568–4572.
[35] H. Xie, H. Lee, W. Youn, M. Choi, Nanofluids containing multiwalled carbon nanotubes and their enhanced thermal properties, J. Appl. Phys. 94 (8) (2003) 4967–4971.
[36] Y.M. Xuan, Q. Li, Heat transfer enhancement of nanofluids, Int. J. Heat Fluid Flow 21 (2000) 58–64.
[37] Y.M. Xuan, W. Roetzel, Conceptions for heat transfer correlation of nanofluids, Int. J. Heat Mass Transfer 43 (2000) 3701–3707.
[38] Y.M. Xuan, Q. Li, Investigation on convective heat transfer and flow features of nanofluids, ASME J. Heat Transfer 125 (2003) 151–155.
[39] Y. Yang, Z.G. Zhong, E.A. Grulke, W.B. Anderson, G. Wu, Heat transfer properties of nanoparticle-in-fluid dispersion (nanofluids) in laminar flow, Int. J. Heat Mass Transfer 48 (2005) 1107–1116.
[40] S.M. You, J.H. Kim, K.H. Kim, Effect of nanoparticles on critical heat flux of water in pool boiling heat transfer, Appl. Phys. Lett. 83 (2003) 3374–3376.
[41] Z. Zhang, F.E. Lockwood, Preparation of stable nanotubes dispersions in liquids, US Patent US6783746B1, August 31, 2004.